

# Fabrication of TiO<sub>2</sub>/Ti nanotube electrode and the photoelectrochemical behaviors in NaCl solutions

Shuhu Xiao · Jiuhui Qu · Huijuan Liu · Xu Zhao · Dongjin Wan

Received: 26 January 2008 / Revised: 25 September 2008 / Accepted: 6 November 2008 / Published online: 4 December 2008  
© Springer-Verlag 2008

**Abstract** Titanium oxide nanotube electrodes were successfully prepared by anodic oxidation on pure Ti sheets in 0.5 wt.% NH<sub>4</sub>F+1 wt.% (NH<sub>4</sub>)<sub>2</sub>SO<sub>4</sub>+90 wt.% glycerol mixed solutions. Nanotubes with diameter 40–60 nm and length 7.4 μm were observed by field emission scanning electron microscope. The electrochemical and photoelectrochemical characteristics of TiO<sub>2</sub> nanotube electrode were investigated using linear polarization and electrochemical impedance spectroscopy techniques. The open-circuit potential dropped markedly under irradiation and with the increase of Cl<sup>-</sup> concentrations. A saturated photocurrent of approximately 1.3 mA cm<sup>-2</sup> was observed under 10-W low-mercury lamp irradiation in 0.1 M NaCl solution, which was much higher than film electrode. Meanwhile, the highest photocurrent in NaCl solution implied that the photogenerated holes preferred to combine with Cl<sup>-</sup>. Thus, a significant synergetic effect on active chlorine production was observed in photoelectrocatalytic processes. Furthermore, the generation efficiency for active chlorine was about two times that using TiO<sub>2</sub>/Ti film electrode by sol–gel method. Finally, the effects of initial pH and Cl<sup>-</sup> concentration were also discussed.

**Keywords** TiO<sub>2</sub>/Ti nanotube electrodes · Chloride ion · Photoelectrochemical behaviors · Active Chlorine · Synergetic effect

## Introduction

Since the photoelectrocatalytic (PEC) process was originally introduced in 1972 [1] as a means to split water, it had been one of the most promising advanced oxidation processes for environmental applications [2–5], which was a combination of electrochemical and photocatalytic treatment processes. It had been demonstrated that applying a bias potential could decrease the recombination rate of photogenerated electron-hole pairs which improved the efficiency of oxidizing organic contaminants. Despite the PEC process usually succeeding to avoid the evolution of oxygen because of the low applied potential, it was strongly restricted by the electrodes, among which, TiO<sub>2</sub> electrodes were widely used. In order to improve the photoelectrocatalytic capability of TiO<sub>2</sub>, preparations of TiO<sub>2</sub> film were extensively studied. TiO<sub>2</sub> films were often prepared using sol–gel method [6], laser calcination [7], electrodeposition [8], or sputtering [9]. Since the first report of self-organized TiO<sub>2</sub> nanotube layers formed by electrochemical titanium anodization in 1999 [10], TiO<sub>2</sub> nanotube electrodes produced in aqueous and organic electrolytes had attracted great interests [11–17] because of their high surface-to-volume ratios, size-dependent properties, and remarkable potential application. As a result, TiO<sub>2</sub> nanotube electrodes had also been introduced and used in the PEC process for contaminant degradation [12, 17].

Chloride ion was usually used as supporting electrolyte in the PEC process. Many researchers had investigated the effect of Cl<sup>-</sup> on the photoelectrocatalytic degradation of pollutants. Some found that the presence of Cl<sup>-</sup> suppressed the degradation rate of organic pollutant, while others found a reverse result. However, to the best of our knowledge, no studies regarding TiO<sub>2</sub> nanotube electrode anodized in organic electrolytes had been reported for environmental

S. Xiao · J. Qu (✉) · H. Liu · X. Zhao · D. Wan  
State key Laboratory of Environmental Aquatic Chemistry,  
Research Center for Eco-Environmental Sciences,  
Chinese Academy of Sciences,  
Beijing 100085, China  
e-mail: jhqu@rcees.ac.cn

S. Xiao · D. Wan  
Graduate School, Chinese Academy of Sciences,  
Beijing 100039, China

application in PEC process, and few systematic studies had been carried out to clarify the role of  $\text{Cl}^-$  especially using  $\text{TiO}_2$  nanotube electrode as photoanode in the PEC process. Herein,  $\text{TiO}_2$  nanotube electrodes were firstly prepared, and then the photoelectrochemical properties were investigated in  $\text{NaCl}$  solutions to find that an enhanced synergetic production of active chlorine was observed by combining electrochemical (EC) with photocatalytic (PC) processes.

## Experimental

### Preparation of $\text{TiO}_2/\text{Ti}$ nanotube electrodes

Titanium sheets (purity, 99.6%; thickness, 0.5 mm) from Beijing Ti Ltd. were used as raw materials. Ti sheets were first ultrasonically cleaned in alcohol and acetone solutions, respectively, and then mechanically polished with different abrasive papers followed by washing with distilled water. The cleaned Ti sheet was submerged in the mixed solution ( $\text{HF}/\text{HNO}_3/\text{H}_2\text{O}$  is 1:4:5 in volume) for 1 min to polish its surface chemically. The  $\text{TiO}_2$  nanotube electrode was fabricated in a cylindrical reactor. 0.5 wt.%  $\text{NH}_4\text{F}$ +1 wt.%  $(\text{NH}_4)_2\text{SO}_4$ +90 wt.% glycerol mixed water solution was used as the electrolyte, and a platinum electrode served as the cathode during the entire process; a potential of 20 V was used in this study. The film electrode was prepared by sol-gel method. The fabricated electrodes were annealed in dry oxygen environment at  $450^\circ\text{C}$  for 2 h to acquire anatase structure.

### Characterization of $\text{TiO}_2/\text{Ti}$ nanotube electrodes

The  $\text{TiO}_2/\text{Ti}$  electrodes were examined by field emission scanning electron microscopy (FE-SEM JSM-6301F) equipped with an energy-dispersive X-ray spectroscopy (EDX). A UV-vis 3010 spectrophotometer (Hitachi, Japan) with an integrating sphere was used to record the diffuse reflectance spectra (DRS) of the samples, and the baseline correction was done using a calibrated sample of barium sulfate.

### Photoelectrochemical experiments

A bench-scale PEC system consisted of a single compartment, semi-cylindrical quartz glass reactor (150 mL in volume) with a standard three-electrode configuration and a 10-W low-pressure mercury lamp with a main emission at 254 nm as an external light source.  $\text{TiO}_2/\text{Ti}$  electrodes ( $6\times 4$  cm) and a Pt wire were separately used as anodes and counter electrode, whereas a saturated calomel electrode (SCE) was used as a reference electrode (all potentials are versus SCE). The electrochemical and photoelectrochemical measurements

were controlled by an EG&G 263A potentiostat (Princeton Applied Research, USA) connecting to a computer. The values of pH were adjusted with 1 M  $\text{NaOH}$  or  $\text{HCl}$  using an Orion 720APLUS Benchtop meter (Thermo Orion, USA), and the content of active chlorine was determined by the DPD (*N,N*-diethyl-*p*-phenylenediamine) colorimetric method [18].

## Results and discussion

### Characterization of $\text{TiO}_2/\text{Ti}$ nanotube electrodes

FE-SEM images of self-assembled  $\text{TiO}_2$  nanotube were shown in Fig. 1 at varying degrees of magnification. It was apparent that the tubes were open from the top. The inner diameters of the nanotubes were mostly around 40–60 nm with the wall about 10 nm and the length reaching approximately  $7.4\ \mu\text{m}$ , which was about 15 times longer than those prepared in  $\text{HF}$  water solutions [17]. Additionally, EDX results (Fig. 1d) showed that the Ti/O mole ratio was

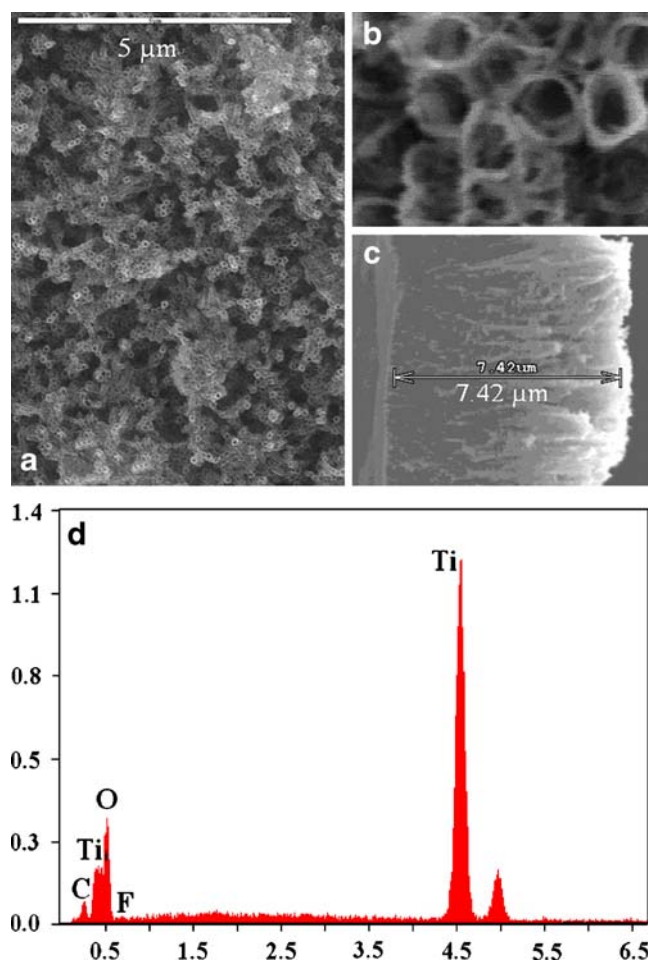


**Fig. 1** FE-SEM images of  $\text{TiO}_2$  nanotube electrodes from the top: **a**  $10,000\times$  magnifications; **b**  $100,000\times$  magnifications; **c** cross-section, and **d** EDX spectra of selected area

estimated to be approximately 1:2 from the ratio of the O peak at 0.523 keV and Ti peak at 4.51 keV.

Optical properties

UV–vis absorbance spectra of TiO<sub>2</sub> nanotube electrode annealed at 450°C was shown in Fig. 2. It revealed that TiO<sub>2</sub> nanotube could absorb the ultraviolet light below 400 nm. The relationship of the absorption coefficient and the incident photon energy of the semiconductor were given by the following equation [19]:

$$\alpha(h\nu) \propto (h\nu - E_g)^n \tag{1}$$

where  $\alpha$  is absorption coefficient,  $h\nu$  is the energy of the incident photon,  $n$  is 0.5 and 2.0 for a direct transition semiconductor and indirect transition semiconductor, respectively. By plotting the graph of  $(\alpha h\nu)$  versus  $h\nu$ , it was possible to determine the nature of transition involved. The extrapolation of straight-line portions of the plot to the zero absorption coefficients gave measurement of energy gap as shown in Fig. 2 inset. A direct band gap value of 3.29 eV was obtained, which was a little higher than that of TiO<sub>2</sub> file electrode [17].

Photoelectrochemical characters

The open-circuit potential was a mixed potential of all the redox potentials in the solution, at the surface and at the interface, and its trend absolutely implied the change of the surface of the electrode [20]. Figure 3 showed the open-circuit potential (OCP) versus UV-irradiation time curves for TiO<sub>2</sub> nanotube electrode in NaCl solutions with different concentrations. The OCP dropped down to much more negative values when the electrode was irradiated with UV light as a result of the

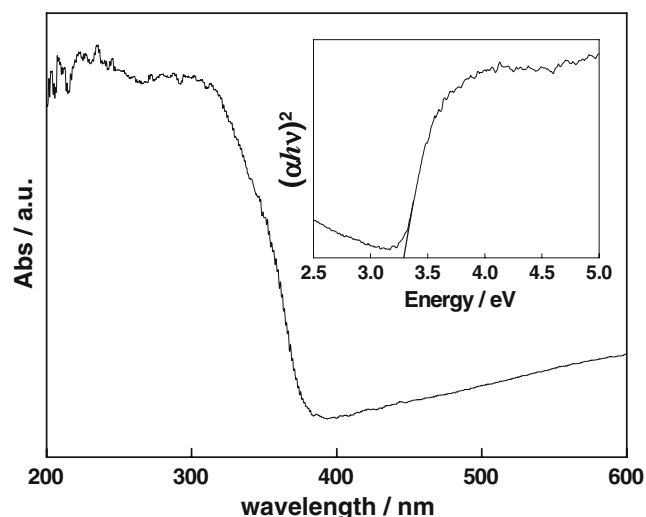


Fig. 2 UV–vis DRS spectra and plots of  $(\alpha h\nu)^2$  versus  $h\nu$  (inset) of TiO<sub>2</sub> nanotube electrode after calcinations at 450 °C

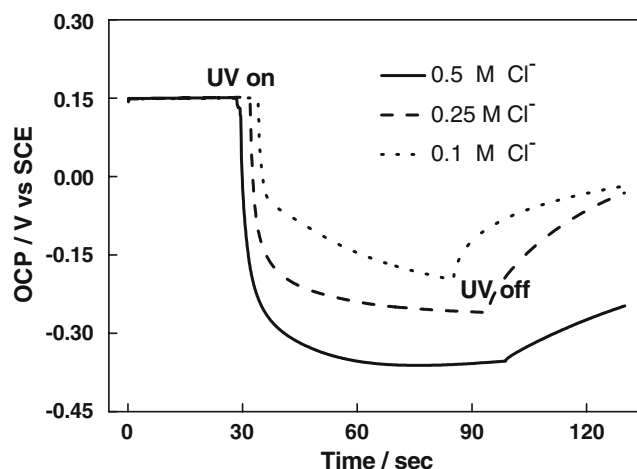


Fig. 3 Variation of open-circuit potential versus time under irradiation in NaCl solutions

sudden generation of e–h pairs. Because of the steady state between generation and depletion of photogenerated carriers, the open-circuit potential trended to stabilize under irradiation, and the unchanging OCP shifted to lower values with the increase of Cl<sup>−</sup> concentrations, which suggested that chloride ions would consume the holes and thus more negative electrons would accumulate on electrode, which reduced the OCP values.

Figure 4 showed the electrochemical impedance spectroscopy (EIS) response of TiO<sub>2</sub> nanotube under dark and irradiation conditions at OCP. It was clear that the size of the arc radius on the EIS Nyquist plot was largely reduced due to the irradiation. Under irradiation, the photogenerated electrons would flow into TiO<sub>2</sub> nanotube electrode and outside circuit. Thus, the interface resistance would reduce and the size of the arc radius on the EIS Nyquist plot reduced. Meantime, the arc radius on the EIS Nyquist plot reflected the rate of electrode reaction, which exhibited that

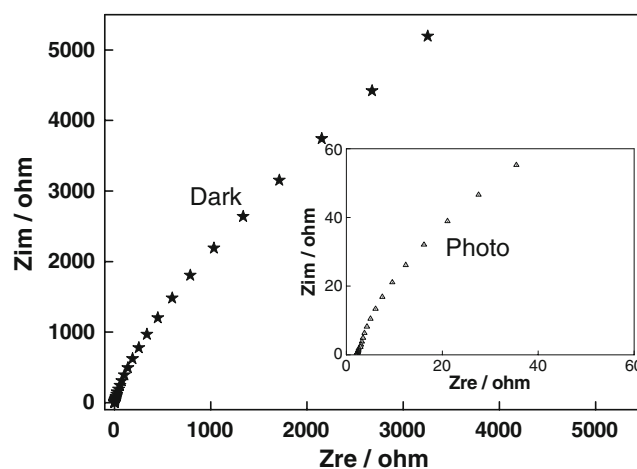
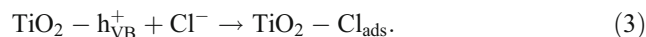


Fig. 4 Effect of UV irradiation on EIS variation of TiO<sub>2</sub> nanotube electrode in 0.5 M NaCl solution

the photoirradiation could increase the reaction rates with the target substances [20–23].

Meanwhile, the  $I$ - $V$  characters of TiO<sub>2</sub> nanotube electrode in NaCl solutions were further measured in the dark and under irradiation as shown in Fig. 5a. When the experiment was carried out in the dark, the anodic current was small and not affected by applied potential below 2 V, which indicated that the electrode possessed a high oxygen and chlorine evolution potentials. It could be seen that an anodic photocurrent arose under UV irradiation when the potential was more positive than -0.3 V. As the applied potential increased, the photocurrent increased linearly and reached to the maximum at 0.5 V. However, a saturation of the photocurrent was observed for the TiO<sub>2</sub> nanotube electrode with potential ranging from 0.5 to 2.0 V, which revealed that the transportation and creation of photoelectrons reached steady state. Meanwhile, photogenerated holes were consumed by hole scavengers or electron donors

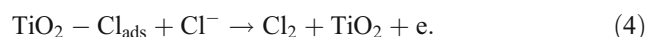
(i.e., Cl<sup>-</sup> ion) in the bulk like Eqs. 2 and 3, which facilitated the continuous creation of photoelectrons.



In addition, photocurrents at 0.5 V in 0.25 M NaNO<sub>3</sub>, NaCl, and NaClO<sub>4</sub> solutions were separately reordered to investigate the selectivity of holes to Cl<sup>-</sup> comparatively. It was clearly observed in Fig. 5b that the photocurrent in NaCl solution was the highest and in NaNO<sub>3</sub> was the lowest. In NaNO<sub>3</sub> solution, the NO<sub>3</sub><sup>-</sup> might absorb the photons of UV light, which resulted in the decrease of light intensity on the electrode. This might be the main reason for the lowest photocurrent. Meanwhile, the photocurrent increased by about two times in NaCl solution compared to that in NaClO<sub>4</sub> solution. Thus, it could be implied that photogenerated holes had a high selectivity to Cl<sup>-</sup> ions.

#### Synergetic production of active chlorine

In the water treatment field, the overall concentration of dissolved chlorine available after the chlorination process was called active chlorine and was given by the summation of three possible species: chlorine (Cl<sub>2</sub>), hypochlorous acid (HClO), and hypochlorite ion (OCl<sup>-</sup>). The production of active chlorine in different processes was presented in Fig. 6. It was obvious that no active chlorine was generated in neither EC nor PC processes. A significant synergetic effect was acquired by combination EC with PC. In the PEC process, the negatively charged chloride ion could be adsorbed on the positively charged photoanode where it might also be subsequently oxidized by the photogenerated holes yielding the oxidized product (Cl<sub>2</sub>), like Eq. 4.



These Cl<sub>2</sub> species spontaneously reacted with water yielding active chlorine. Furthermore, it was also easily seen that the TiO<sub>2</sub> nanotubes and film electrodes exhibited different photoelectrocatalytic activity. TiO<sub>2</sub> nanotube electrode produced about two times of active chlorine as film electrode. It might be attributed to the difference of band gap energy and specific surface area between the nanotubes and the film. The band gap energy of TiO<sub>2</sub> nanotube was higher, indicating that more powerful photocarriers would be produced under irradiation; in the meantime, TiO<sub>2</sub> nanotubes had larger specific surface area than TiO<sub>2</sub> film that could adsorb more Cl<sup>-</sup>, which could be inferred by the  $I$ - $V$  characters above.

#### Effect of the initial pH

To investigate the effect of initial pH on the production of active chlorine, the solutions were adjusted from pH 2 to

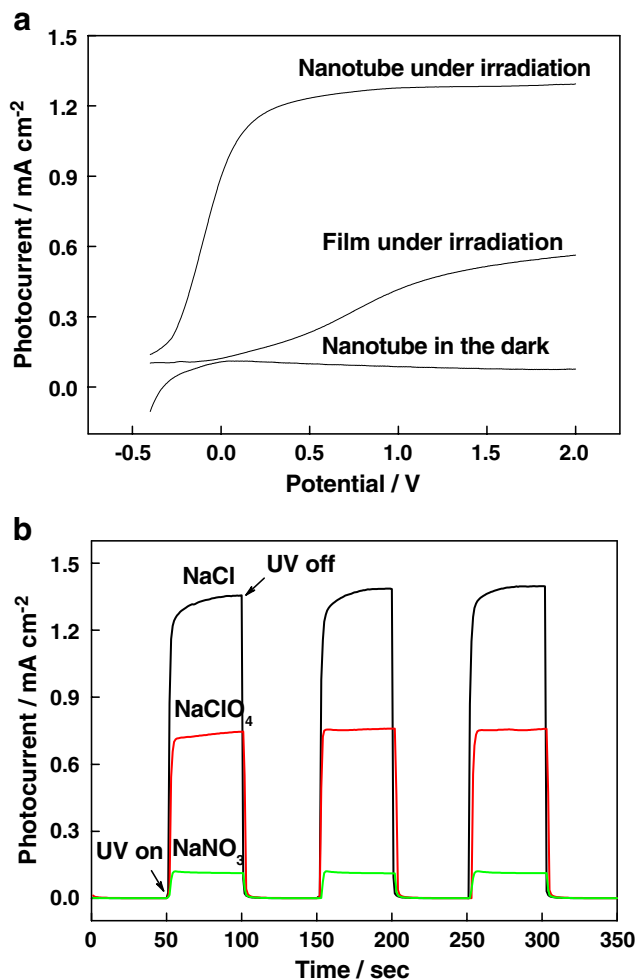


**Fig. 5** a  $I$ - $V$  characters of different electrodes in 0.1 M NaCl solution. b Current variation with UV on and off in 0.25 M NaCl, NaClO<sub>4</sub> and NaNO<sub>3</sub> solutions at applied potential 0.5 V

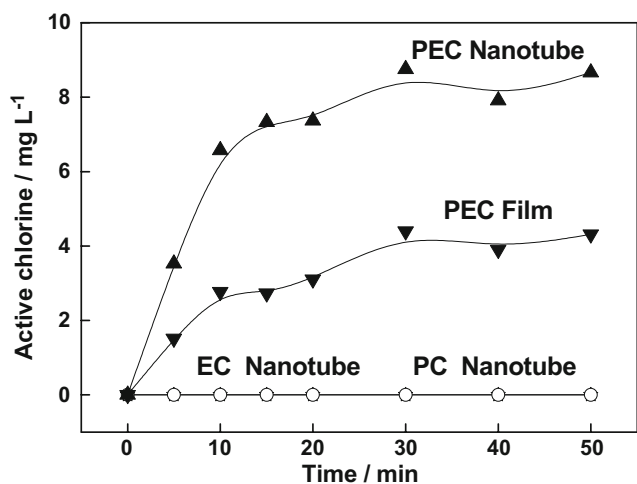


**Fig. 6** Production of active chlorine at different processes: initial  $\text{Cl}^-$  concentration=0.08 M, applied potential=0.5 V, 15-W low-pressure mercury lamp

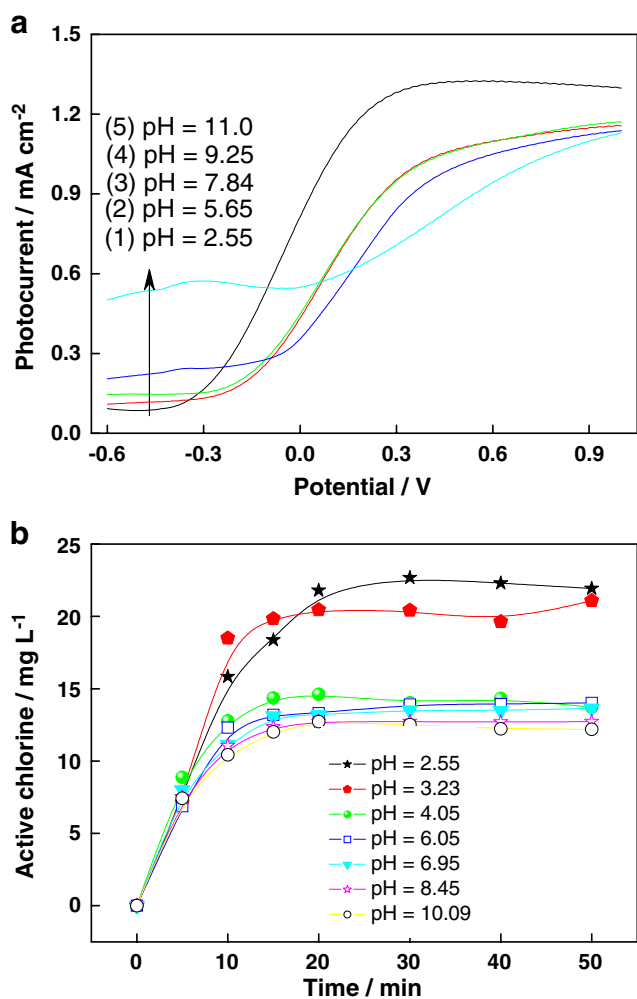


**Fig. 7** Photocurrent (a) and production of active chlorine (b) variation with irradiation at different pH. Scan rate=50  $\text{mV s}^{-1}$ , initial  $\text{Cl}^-$  concentration=0.08 M, applied potential=0.5 V, 15-W low-pressure mercury lamp

11. The dependences of photocurrent and active chlorine formation on the pH values of the solution were presented in Fig. 7. It was obvious that the saturated photocurrent was much higher at pH 2.55, and it decreased gradually with the increase of pH values (Fig. 7a). Not surprisingly, the generation of active chlorine was similar to that of photocurrent versus pH values, as shown in Fig. 7b. The pH of solution could influence the PEC production of active chlorine through the following processes: (a)  $\text{TiO}_2$  flat-band potential variation, (b) adsorption isotherm of electroactive species (the adsorption of electroactive species was governed by Langmuir adsorption equilibrium equation) [24], (c) photoelectrochemical oxidation of water and  $\text{OH}^-$  ion competing with  $\text{Cl}^-$  ion [25], (d) the forms of active chlorine variation, and (e) byproduct formation of  $\text{ClO}_3^-$  in basic solution [26]. Thus, the  $\text{TiO}_2$  was positively charged and adsorbed the negatively charged chloride ions to react with photogenerated holes predominantly, and the main component of active chlorine,  $\text{HClO}$ , would not be oxidized to  $\text{ClO}_3^-$  in acid solution, which was beneficial to the photoelectrocatalytic production of active chlorine.

Effect of chloride concentration

The photoelectrocatalytic production of active chlorine as a function of the concentration of NaCl was investigated using solutions at pH 3.0 and the applied potential of 0.5 V as shown in Fig. 8. It could be seen that higher active chlorine production was acquired by an increase in  $\text{Cl}^-$  concentrations. Nevertheless, further increasing the chloride concentration above 0.1 M promoted little in the conversion of active chlorine, thereby showing a limiting rate in the

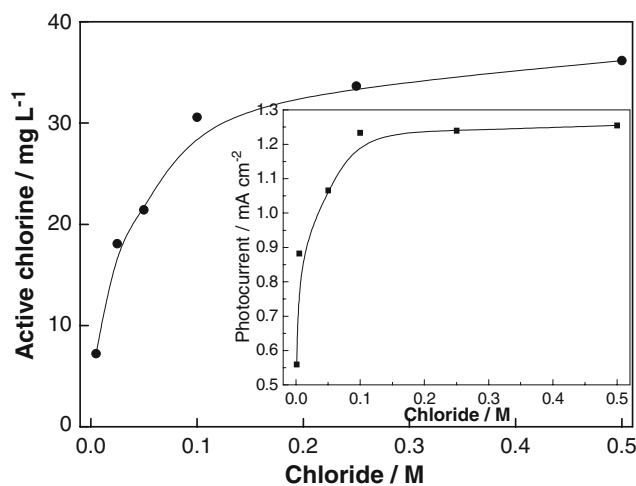


**Fig. 8** The effect of initial  $\text{Cl}^-$  concentrations on photoelectrocatalytic production of active chlorine and photocurrents (inset). Initial pH=3.0, applied potential=0.5 V, time=25 min, 15-W low-pressure mercury lamp

oxidation of  $\text{Cl}^-$  ions. The same results were obtained to the photocurrent at 0.5 V with the increase of chloride ion (Fig. 8, inset). As electron donors of photogenerated holes, chloride ions accelerated the separation of electron-hole pairs. At lower concentration of chloride, the electron-hole pairs generated at a steady-state rate could recombine preferentially, since chloride ions were weakly adsorbed to the electrode surface restricting by mass transfer (i.e., diffusion-controlled process). However, at higher chloride concentration above 0.1 M, it was likely that the adsorption effect would predominate, avoiding charge recombination. Photocurrent was limited by the electrode/solution interfacial reactions and the photogenerated holes capture process. Since the photogenerated holes were constant at certain conditions, further increasing the concentration of  $\text{Cl}^-$  could not enhance the photocurrent, nor did active chlorine.

## Conclusions

Titanium oxide nanotubes with diameter 40–60 nm and length 7.4  $\mu\text{m}$  were successfully prepared by anodic oxidation on a pure Ti sheet in 0.5 wt.%  $\text{NH}_4\text{F}$ +1 wt.%  $(\text{NH}_4)_2\text{SO}_4$ +90 wt.% glycerol mixed solution. From darkness to the photoirradiation, the OCP decreased markedly as a result of the accumulation with photogenerated electrons. EIS spectra results exhibited that the photoirradiation could increase the reaction rates with  $\text{Cl}^-$ . The electrons in the conduction band would flow via an external circuit to the cathode under irradiation and a bias potential, which resulted in a saturated photocurrent of 1.3  $\text{mA cm}^{-2}$ . Meanwhile, the holes possessed a high selectivity to  $\text{Cl}^-$  ions. Thus, a significant synergetic production of active chlorine was acquired in PEC processes, and the efficiency was about two times that using  $\text{TiO}_2/\text{Ti}$  film electrode by sol-gel method. Additionally, a maximum of active chlorine could be acquired at pH 2.5–3.2 with about 0.1 M  $\text{Cl}^-$ .

**Acknowledgments** This work was supported by the Funds for Creative Research Groups of People's Republic of China (no. 50621804) and the National Natural Science Foundation of China (no. 50538090).

## References

- Fujishima A, Honda K (1972) *Nature* 238:37. doi:10.1038/238037a0
- Zhao X, Zhu Y (2006) *Environ Sci Technol* 40:3367. doi:10.1021/es052029e
- Li XZ, Liu HL, Yue PT (2000) *Environ Sci Technol* 34:4401. doi:10.1021/es000939k
- Osugi ME, Umbuzeiro GA, Anderson MA, Zaroni MVB (2005) *Electrochim Acta* 50:5261. doi:10.1016/j.electacta.2005.01.058
- Cameiro PA, Osugi ME, Sene JJ, Anderson MA, Zaroni MVB (2004) *Electrochim Acta* 49:3807. doi:10.1016/j.electacta.2003.12.057
- Egerton TA, Janus M, Morawski AW (2006) *Chemosphere* 63:1203. doi:10.1016/j.chemosphere.2005.08.074
- Li J, Li L, Zheng L, Xian Y, Jin L (2006) *Electrochim Acta* 51:4942. doi:10.1016/j.electacta.2006.01.037
- Li G, Qu J, Zhang X, Ge J (2006) *Water Res* 40:213. doi:10.1016/j.watres.2005.10.039
- He C, Li XZ, Graham N, Wang Y (2006) *Appl Catal A* 305:54. doi:10.1016/j.apcata.2006.02.051
- Zwilling V, Aucouturier M, Darque-Ceretti E (1999) *Electrochim Acta* 45:921. doi:10.1016/S0013-4686(99)00283-2
- Macák JM, Tsuchiya H, Schmuki P (2005) *Angew Chem Int Ed* 44:2100. doi:10.1002/anie.200462459
- Xie Y (2006) *Electrochim Acta* 51:3399. doi:10.1016/j.electacta.2005.10.003
- Macak JM, Sirotna K, Schmuki P (2005) *Electrochim Acta* 50:3679. doi:10.1016/j.electacta.2005.01.014
- Macak JM, Tsuchiya H, Taveira L, Aldabergerova S, Schmuki P (2005) *Angew Chem Int Ed* 44:7463. doi:10.1002/anie.200502781
- Bauer S, Kleber S, Schmuki P (2006) *Electrochem Commun* 8:1321. doi:10.1016/j.elecom.2006.05.030
- Mor GK, Varghese OK, Paulose M, Grimes CA (2005) *Adv Funct Mater* 15:1291. doi:10.1002/adfm.200500096
- Quan X, Yang S, Ruan X, Zhao H (2005) *Environ Sci Technol* 39:3370. doi:10.1021/es048684o
- APHA AWWA, WEF (2005) *Standard methods for the examination of water and wastewater*, 21st edn. American Public Health Association, American Water Works Association, Water Environment Federation, Washington, DC
- Pankove LI (1970) *Optical processes in semiconductors*. Dover, New York
- Li MC, Shen JN (2006) *J Solid State Electrochem* 10:980. doi:10.1007/s10008-005-0043-5
- Qu J, Zhao X (2008) *Environ Sci Technol* 42:4934. doi:10.1021/es702769p
- Liu H, Cheng S, Wu M, Wu H, Zhang J, Li W, Cao C (2000) *J Phys Chem A* 104:7016. doi:10.1021/jp000171q
- Wu X, Ma H, Chen S, Xu Z, Sui A (1999) *J Electrochem Soc* 146:1847. doi:10.1149/1.1391854
- Ohtsuka T, Otsuki T (1999) *J Electroanal Chem* 473:272–278. doi:10.1016/S0022-0728(99)00238-7
- Selcuk H, Anderson MA (2005) *Desalination* 176:219. doi:10.1016/j.desal.2004.10.016
- Zhao X, Liu M, Zhu Y (2007) *Thin Solid Films* 515:7127. doi:10.1016/j.tsf.2007.03.025